Indian Journal of Chemical Technology
Vol. 27, January 2020, pp. 9-17

Optical and anti-oxidant application of zinc doped cadmium sulfide nanoparticle

C Selvakumar*[1, 2] & M Deepa[3]

[1]Sri Sairam Engineering College, Saileonagar, Tambaram, Chennai 600 044, India

[2]Research and Development, Bharathiar University, Coimbatore 641 046, India

[3]Muthurangam Goverment Arts College, Oteri, Vellore 632 002, India

E-mail: selvakumar.chem@sairam.edu.in

Received 16 February 2018; accepted 10 December 2018

Present work explains about optical and oxidant activity of zinc doped cadmium sulfide nanoparticle. Compare with undoped cadmium sulfide, zinc doped nanoparticles have different results in IR, SEM, TEM and XRD. EDAX image shows the crystalline arrangement of nanoparticles. Anti-oxidant activity describes using DHHP's radical scavenging method and optical relation determine by Tauc's equation.

Keyword: Band gap, Scavenging test, Semi-conductor, Cadmium sulfide nanoparticles

Sustainable development is the recent and important way for our future generation with green synthetic method, because the effect of pollution have poisonous effect among peoples. Solar cells are the best alternative way for generating energy from fossil fuel. It is a semiconductor device that converts the energy of sunlight into electrical energy, based on photo voltaic effect. Solar cells do not use chemical reaction to produce electric power, and they have no moving parts. Photovoltaic solar cells are thin silicon disks that convert sunlight into electricity. These disks act as energy sources for a varied variety of uses, including calculators and other small devices, telecommunications, rooftop panels on individual houses, and for lighting, pumping, and medical refrigeration for villages in developing countries. In large arrays, which may contain many thousands of individual cells, they can function as central electric power stations analogous to nuclear, coal-, or oil-fired power plants. Arrays of solar cells are also used to power satellites, because they have no moving parts that could require service or fuels that would require renewable, solar cells are ideal for providing power in space. Most photovoltaic cells consist of a semiconductor p and n type, in which electron-hole pairs formed by absorbed radiation are separated by the internal electric field in the junction to generate a current, a voltage, or both, at the device terminals. Under open-circuit conditions (current $I = 0$) the terminal voltage rises with ricing light intensity, and under short-circuit conditions (voltage $V = 0$) the magnitude of the current increases with increasing light intensity. When the current is negative and the voltage is positive, the photovoltaic cell delivers power to the external circuit. The usable voltage from solar cells depend on the semiconductor material. In silicon it amounts to approximately 0.5 V. Terminal voltages is only weakly dependent on light radiation, while the current intensity increases with higher luminosity. A 100 cm^2 silicon cell, for example, reaches a maximum current intensity of approximately 2 A when radiated by 1000 W/m^2. The output (product of electricity and voltage) of a solar cell is temperature dependent. Higher cell temperatures lead to lower output, and hence to lower efficiency. The level of efficiency indicates how much of the radiated quantity of light is converted into usable electrical energy. Nano composites are used to prepare solar cells with high band gap. Especially copper and zinc doped nanoparticle are shows good semiconducting properties. Knowing about nanomaterial are most important for future development of energy storage devices. The DPPH is a stable free radical and is widely used to assess the radical scavenging activity of antioxidant component. DPPH scavenging activity was measured using the method with slight modifications. 1,1-diphenyl-2-picrylhydrazyl (DPPH) methanolic solution (0.135 mM) was used. DPPH concentration is reduced by the existence of an antioxidant at 517 nm and the

absorption gradually disappears with time. This method is based on the reduction of DPPH in methanol solution in the presence of a hydrogen donating antioxidant due to the formation of the non-radical form of DPPH. Briefly, 0.135 mM solution of DPPH in methanol was prepared, and 180 µL of this solution was added to 20 µL of the solution of all manganese doped zinc sulfide nanoparticle samples at different concentrations.

5 mg manganese doped zinc sulfide were dissolved in 1 mL of water to obtain the aliquot of manganese doped zinc sulfide nanoparticles (10, 50, 100, 500 and 1000 µg/mL). The diluted working solutions of the test manganese doped zinc sulfide nanoparticles were prepared in water. The mixtures were kept at room temperature for 30 min. Ascorbic acid was used as a positive control (standard) and methanol as a blank.The experiments were performed in triplicate and percentage scavenging activity was calculated using following equation ,

% of Scavenging activity =

[(Absorbance control − Absorbance sample)/Absorbance control] × 100

The UV-visible spectrum of ZnS and CuS was recorded using UV spectrophotometer in the range 200-900 nm. The spectrum gives information about the structure of molecules and optical energy band gap of molecules, because the absorption of UV and visible light involves promotion of the electron from ground state to higher states. The observed nature of absorption in the visible region is a desirable property for NLO (Non-Linear optical) applications. The crystal shows good optical transmittance up to 14% in the entire region. It shows lower cut off ranges from 200-500 nm. This reveals that in the grown crystal the absorption is almost absent in the visible region due to its high transparency. The band gaps can be calculated via UV-V is spectroscopy using Tauc's Plots. The optical absorption coefficient (α) was calculated by using the equation,

$$\alpha = \frac{2.303(1/T)}{t}$$

where 'T' is the transmittance and't' is thickness of the crystal, Optical band gap (Eg) was assessed from the transmission spectra and optical absorption coefficient (α) near the absorption edge is given by equation ,

$$(\alpha h\nu)^2 = A(h\nu - E_g)$$

where 'A' is a constant, 'Eg' is the optical band gap, 'h' is Planck constant, and 'υ' is the frequency of incident photons. The band gap of zinc and copper sulfide crystal was estimated by plotting $(\alpha h\upsilon)^2$ versus hυ extrapolating the linear portion near onset of absorption edge to the energy axis. From the graph, the value of band gap was found. The term "band gap" refers to the energy difference between the top of the valence band to the bottom of the conduction band, electrons are able to jump from one band to another. In order for an electron to jump from a valence band to a conduction band, it requires a specific minimum amount of energy for the transition, the band gap energy. Measuring the band gap is important in the semiconductor and nanomaterial industries. The band gap energy of insulators is large (> 5eV), but lower for semiconductors (< 3.5eV). The band gap properties of a semiconductor can be controlled by using different semiconductor alloys. An alternative strategy is to use layers of different materials coated on to the silicon base material. This is employed in the solar industry in the construction of photovoltaic (PV) solar cells. The band gap is important as it determines the portion of the solar spectrum, which photovoltaic cell absorbs. Much of the solar radiation reaching the earth is comprised of wavelengths with energies greater than the band gap of silicon. These higher energies will be absorbed by the solar cell, but the difference in energy is converted into heat rather than into usable electrical energy. Consequently, unless the band gap is controlled, the efficiency of the solar cell will be poor. Using layers of different materials with different band gap properties is a proven way to maximize the efficiency of solar cells. In the semiconductor and nanomaterial industries, titanium dioxide (TiO_2) is added as an ingredient to coatings.

Preparation nanoparticles with various composition

The various composition of cadmium acetate, zinc chloride and sodium sulfide. Calculated amount of various composition of cadmium acetate(X) and zinc chloride (Y) were dissolved in a beaker containing 50 mL of de-ionized water and 50 mL of methanol. The above mixture was kept in a magnetic stirrer for stirring and simultaneously weighted composition of sodium sulfide (Z) was dissolved in 50 mL of deionized water and 50 mL of methanol along with 0.5 gms of poly vinyl alcohol (PVA) were added through burette drop by drop. The stirring were continued for almost half an hour until the fine

precipitate of zinc doped cadmium sulfide nano particles was obtained. Then precipitate were filtered off and washed several times with methanol to purify the sample. The content was then placed in microwave oven for evaporation. At last fine yellow precipitate was obtained, indicates formation of nano composites. Various composition of NP's had been prepared with different molecular mass ratio as shown in Table 1.

Result and Discussion

FTIR spectral analysis for zinc doped cadmium sulfide [Zn:CdS]

When compared with undoped cadmium sulfide, doped cadmium sulfide have admirable characteristics. IR analysis of undoped and doped cadmium sulfide nanoparticles are discussed below. The FT-IR spectra of zinc doped cadmium sulfide ($Zn_{2.5}$:$Cd_{6.6}$ $S_{0.9}$) are shown in Fig. 1. The assignment of the peaks in the FT-IR are 3602, 1539, 1400 and 611 cm^{-1}. Comparison of the FT- IR spectra of undoped zinc nanoparticles and that of zinc doped cadmium sulfide nanoparticles clearly show the differences in them, which clearly demonstrate the synthesis of doped Zn nanoparticle.Using peaks we can explain the functional group of compounds. 3602 cm^{-1} shows strong peak due to –OH stretching of methanol used as a solvent along with water, 1539 cm^{-1} designates sharp bending vibrational peak of the water (H-O-H) absorbed on the surface of cadmium sulfide, 1400 cm^{-1} indicates C-H stretching vibration of methanol used as a solvent and 611 cm^{-1} peaks demonstrates cadmium sulfide bond stretching. FT-IR shows peaks at 3331, 1539, 1404, 1330, 1101, and 611 cm^{-1}. IR peaks of $Zn_{6.2}$:$Cd_{2.4}S_{1.4,}$ present compound shows strong peak at 3331 cm^{-1} due to –OH stretching of methanol, which was used as a solvent. 1539 cm^{-1} designates sharp bending (H-O-H) vibrational peak of the water absorbed on the surface of cadmium sulfide, 1330 cm^{-1} indicates C-H stretching vibration of methanol used as a solvent and 611 cm^{-1} peaks demonstrates cadmium sulfide bond stretching. Fourier Transform Infra-Red spectra shows in Fig. 2. The assignment of the peaks in the FT-IR are 3130,1529, 1402, 1107 and 613 cm^{-1}. Using FTIR peaks can explain the functional group of compounds. 3130 cm^{-1} shows strong peak due to –OH stretching of methanol used as a solvent, 1529 cm^{-1} designates sharp bending (H-O-H) vibrational peak of the water absorbed on the surface of cadmium sulfide, 1402 cm^{-1} indicates C-H stretching vibration of methanol used as a solvent and 613 cm^{-1} peaks demonstrates cadmium sulfide bond stretching. Fourier transform infra-red spectra of sample III were shows in Fig. 3

Table 1 — Composition of Zinc doped cadmium sulfide nanoparticles

S.No.	Sample code	Sample composition	X gram of $Cd(COOH)_2$	Y gram of $ZnCl_2$	Z gm of Na_2S
1.	I	$Zn_{2.5}$:$Cd_{6.6}$ $S_{0.9}$	6.6	2.5	0.9
2.	II	$Zn_{2.8}$:$Cd_{6.2}S_{1.0}$	6.2	2.8	1.0
3.	III	$Zn_{3.2}$:$Cd_{5.8}S_{1.1}$	5.8	3.2	1.1

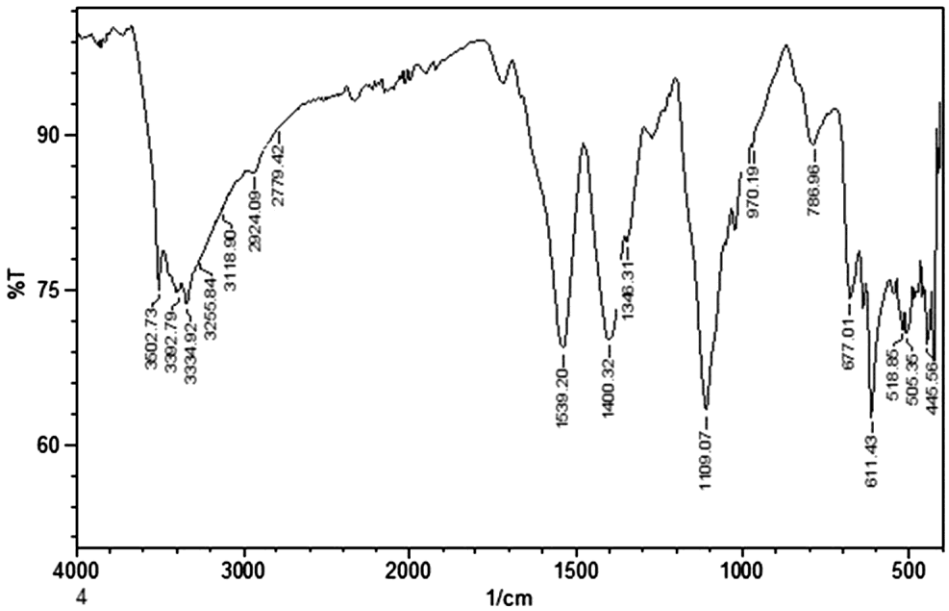

Fig. 1 — FTIR Interpretation for $Zn_{2.5}$:$Cd_{6.6}$ $S_{0.9}$ nanoparticle

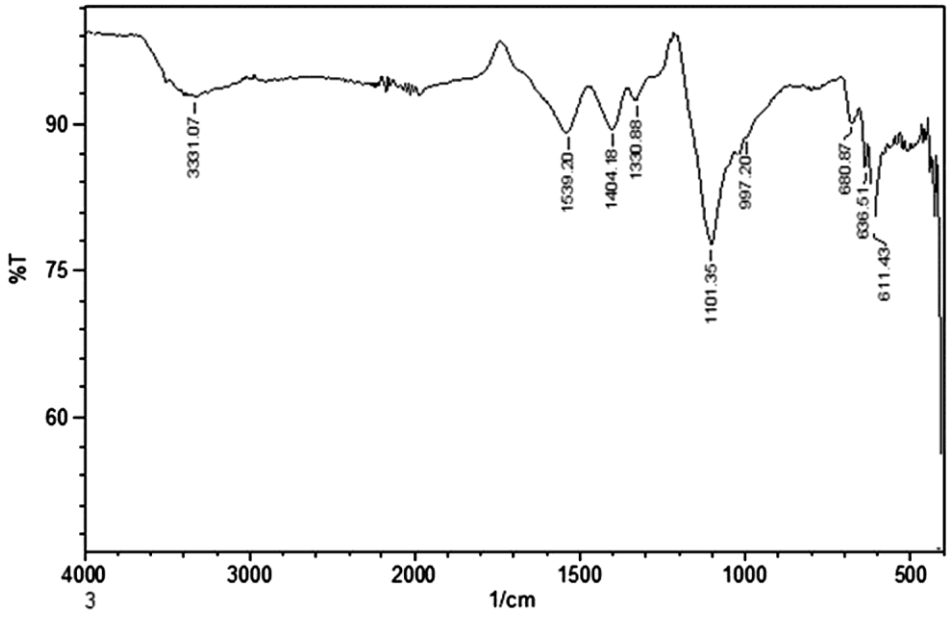

Fig. 2 — FTIR Interpretation for $Zn_{2.5}$:$Cd_{6.6}$ $S_{0.9}$ nanoparticle

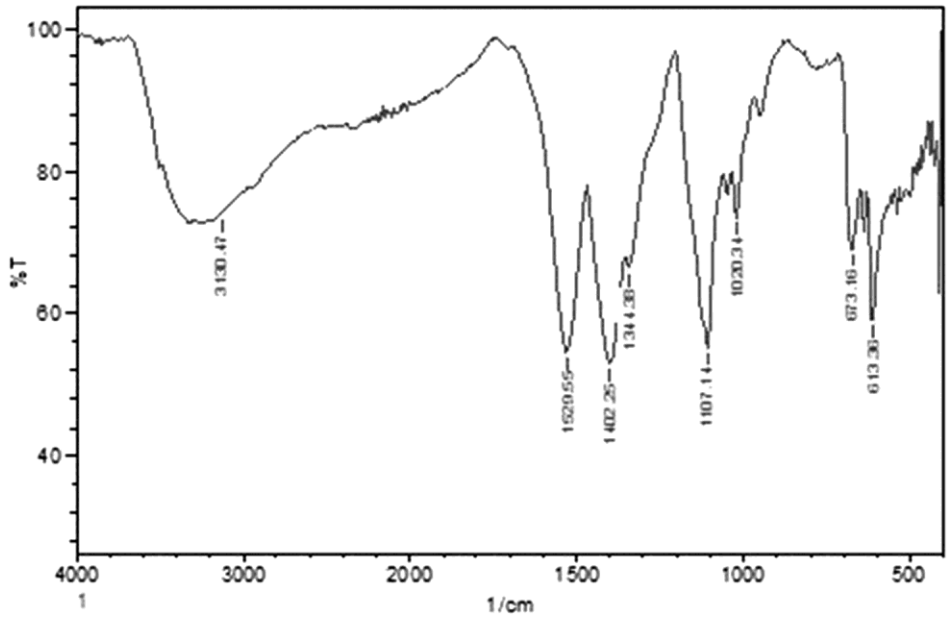

Fig. 3 — FTIR Interpretation for $Zn_{2.5}$:$Cd_{6.6}$ $S_{0.9}$ nanoparticle

XRD pattern of zinc doped cadmium sulfide nanoparticles

Figure 4 denoted powder XRD pattern of the zinc doped cadmium sulfide nanoparticles. XRD pattern was indicated that, the product is Zn doped with CdS nanoparticle sample is not only due to adsorption but also due to covalent bond formation. The 2θ values obtained for $Zn_{2.5}$:$Cd_{6.6}$ $S_{0.9}$ are 8, 12 and 18. According to the full width at half maximum of the diffraction peaks, the average size of the particles could be estimated from the Scherer equation to be about 2, 3 and 4.5 nm. Using this detail can prove that, the compound have crystalline structure and have regular arrangement in crystal lattice.

The 2θ values obtained for $Zn_{3.2}$:$Cd_{5.8}S_{1.1}$ are 26, 33 and 44. According to the full width at half maximum of the diffraction peaks, the average size of the particles could be estimated from the Scherer equation to be about 6.5, 8.2 and 11 nm. Using this detail we can conclude that, the compound have crystalline structure and have regular arrangement in crystal

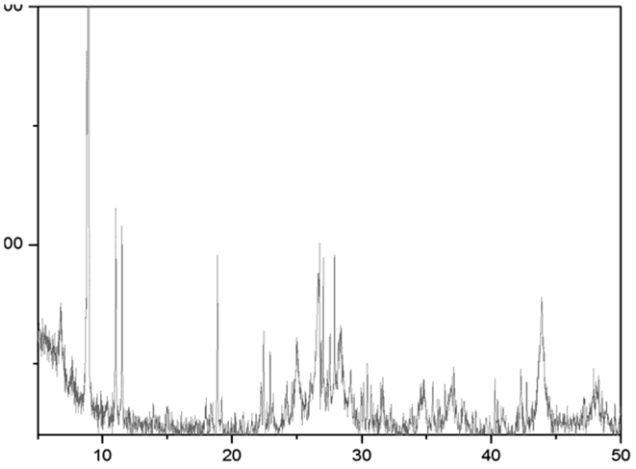

Fig. 4 — XRD interpretation for $Zn_{2.5}$:$Cd_{6.6}$ $S_{0.9}$ nanoparticle

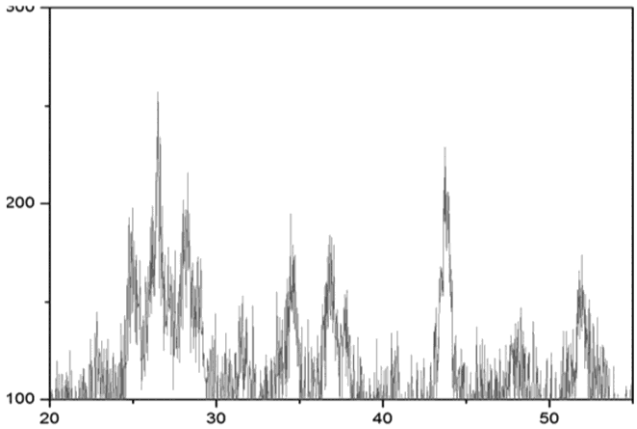

Fig. 5 — XRD interpretation for $Zn_{2.8}$:$Cd_{6.2}S_{1.0}$ nanoparticle

lattice. Figure 5 denoted powder XRD pattern of the zinc doped cadmium sulfide nanoparticles. This indicates that the product is composed Zn doped with CdS nanoparticle is not only due to adsorption but also due to covalent bond formation. Figure 6 denoted powder XRD pattern of the zinc doped cadmium sulfide nanoparticles. According to the full width at half maximum of the diffraction peaks, the average size of the particles could be estimated from the Scherer equation was found to be about 7.2, 12.5 and 14.5 nm.

Using this detail we can conclude that, the compound have crystalline structure and have regular arrangement in crystal lattice. Based on JCPDS analysis zinc doped cadmium sulfide nanoparticles shows hexagonal arrangement and card number. 41-1049.

SEM analysis

The operating principles of SEM are very similar to that of TEM, such as a high-voltage electron beam is used to excite the sample. Morphology, shape and

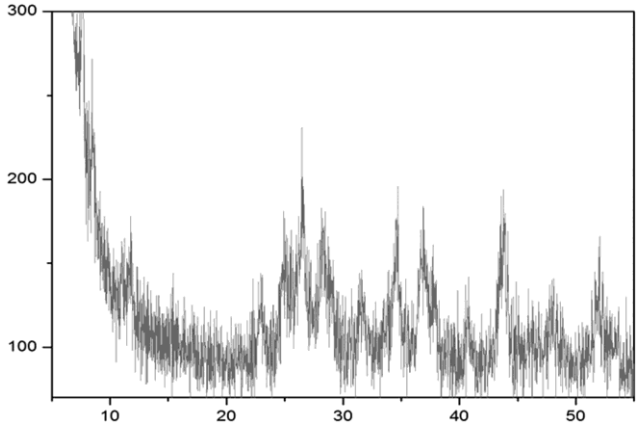

Fig. 6 — XRD interpretation for $Zn_{3.2}$:$Cd_{5.8}S_{1.1}$ nanoparticle

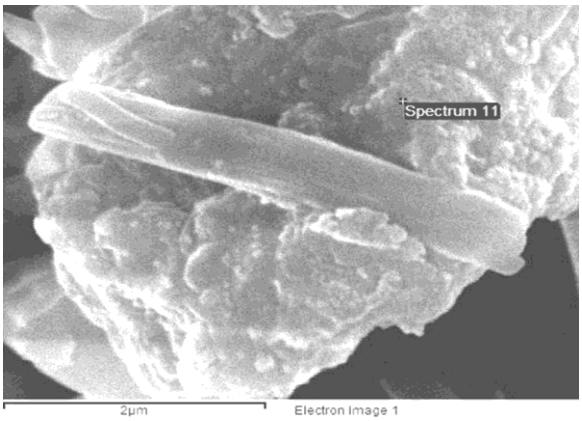

Fig. 7 — SEM pattern of $Zn_{2.5}$:$Cd_{6.6}$ $S_{0.9}$ nano particles

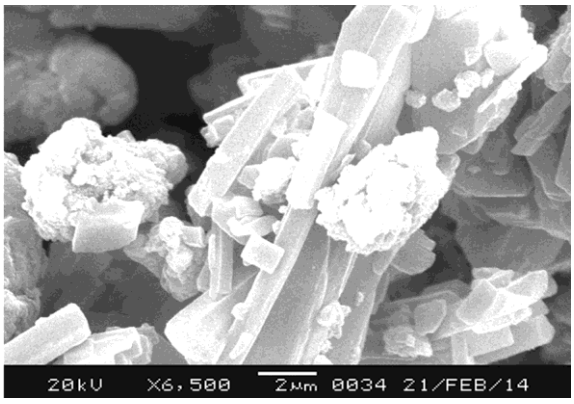

Fig. 8 — SEM pattern of $Zn_{2.8}$:$Cd_{6.2}S_{1.0}$ nano particles

size of the nanoparticles was investigated by scanning electron microscope recorded at different magnifications. SEM image of sample I, II and III are shown in Figs. 7, 8 and 9. It is evident that the structure of the nanoparticles appears as globular shape with different sizes[18]. It is apparently understood that aggregation of the nanoparticles is controlled by doping with different concentration of

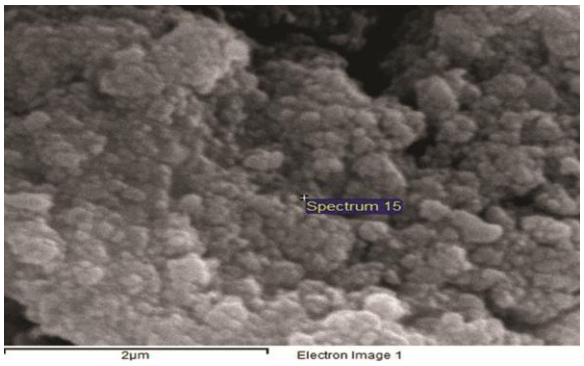

Fig. 9 — SEM pattern of $Zn_{3.2}$:$Cd_{5.8}S_{1.1}$ nano particles

cadmium. We observed that from SEM analysis, the particles are uniformly distributed. The SEM images of Zn doped CdS nanoparticle confirms the existence of very small crystalline nanoparticle.

The particle size and distribution of nanoparticle mainly depends upon the doping concentration. The Zn doped with CdS nanoparticle, the structure of CdS is flake like structure. When the concentration of Zn is increased, the structure of CdS becomes cluster form.

TEM and SEAD analysis

Morphologies of nanoparticles can also be explained by the TEM image. It displays rough area on the surface of zinc doped cadmium sulfide compound, which explains the catalysis application of product[19]. TEM also explain the size of zinc doped cadmium sulfide nanoparticles lies between 2-14 nm. It displays crystalline arrangement of product by appearing lines in TEM figure 10 and 11.

SEAD shows (Fig. 12) particle's crystalline arrangement of nano composites. The selected area electron diffraction (SAED) patterns were recorded using Philips, Technai-20 transmission electron microscopy using CCD with electron source as W (tungsten) emitter and LaB_6, having accelerating voltage 200 kV. The pattern clearly shows rings, substantiating polycrystallinity of the samples. The value obtained from TEM are in good agreement with the values obtained from XRD.

Application of zinc doped cadmium sulfide

UV-Visible spectroscopic analysis

Spectrophotometry investigates the absorption of the different substances between the wavelength limits 190 nm and 780 nm (visible spectroscopy is restricted to the wavelength range of electromagnetic radiation detectable by the human eye, that is above

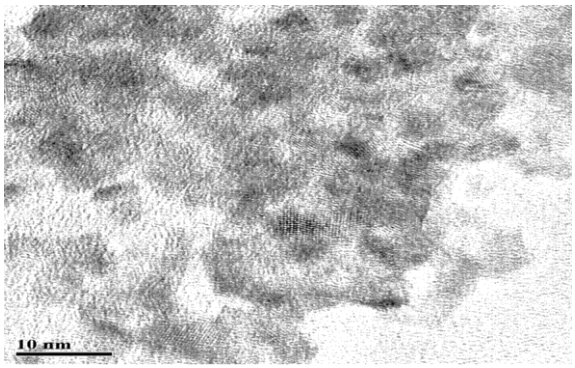

Fig. 10 — TEM pattern of $Zn_{2.5}$:$Cd_{6.6}S_{0.9}$ nano particles

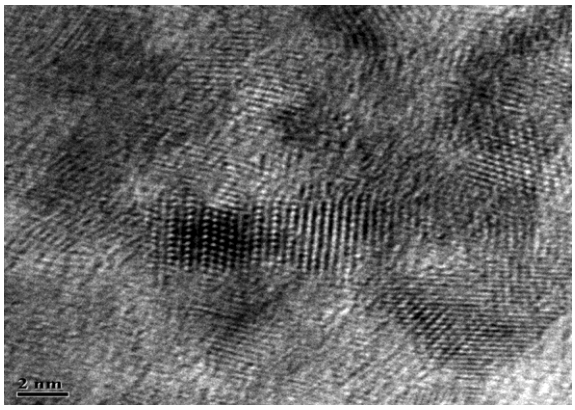

Fig. 11 — TEM pattern of $Zn_{3.2}$:$Cd_{5.8}S_{1.1}$ nano particles

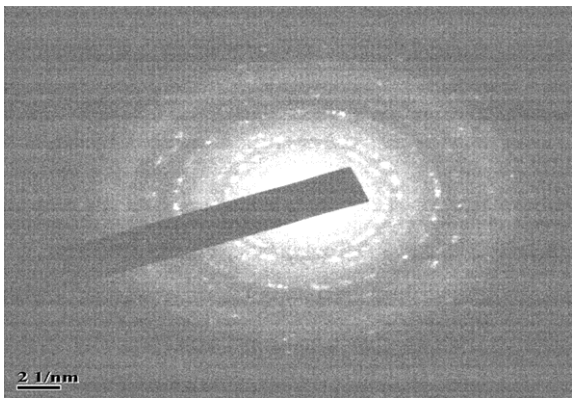

Fig. 12 — SEAD image of Zn:CdS nano particles

360 nm, ultraviolet spectroscopy is used for shorter wavelengths). In this wavelength range the absorption of the electromagnetic radiation is caused by the excitation (i.e. transition to a higher energy level) of the bonding and non-bonding electrons of the ions or molecules. A graph of absorbance against wavelength gives the sample's absorption spectrum. Spectrophotometry is used for both qualitative and quantitative investigations of samples. The wavelength at the maximum of the absorption

band gives information about the structure of the molecule or ion and the extent of the absorption is proportional to the amount of the species absorbing the light.

Figure 13 shows UV-Visible spectrum of zinc doped cadmium sulfide nanoparticles. The wavelength of samples is 230 nm, which is blue shift. This is because of quantum confinement effect. Also a sight red shift has been observed in the absorption edge on doping the nanoparticles with high concentration of zinc.

Optical band gap calculated by Tauc relation and above graph. Band gap value around 5.25 eV. So it not act as a semiconductor, but it shows higher band gap value. That means zinc nanoparticles have higher capacitance application. It can explain by above graph (Fig. 14).

Anti-oxidant activity of zinc doped cadmium sulfide nanoparticles [Zn:CdS]

The DPPH is a stable free radical and is widely used to assess the radical scavenging activity of antioxidant component. DPPH scavenging activity was measured using the method with slight modifications. 1,1-diphenyl-2-picrylhydrazyl (DPPH) methanolic solution (0.135 mM) was used. DPPH concentration is reduced by the existence of an antioxidant at 517 nm and the absorption gradually disappears with time. Briefly, 0.135 mM solution of DPPH in methanol was prepared, and 180 µL of this solution was added to 20 µL of the solution of all zinc doped cadmium sulfide nanoparticle samples at different concentrations Fig. 15. 5 mg zinc doped cadmium sulfide were dissolved in 1 mL of HPLC water to obtain the aliquot of zinc doped cadmium sulfide nanoparticles (10, 50, 100, 500 and 1000 µg/mL). The diluted working solutions of the test zinc doped cadmium sulfide NPs were prepared in HPLC water (sonicated for 10 min). The mixtures were kept at room temperature for 30 min Ascorbic acid was used as a positive control (standard) and methanol as a blank. The experiments were performed in triplicate and percentage scavenging activity was calculated using following equation,

$$\% \text{ of Scavenging activity} = [(\text{Absorbance control} - \text{Absorbance sample})/\text{Absorbance control}] \times 100$$

All experiments were repeated in triplicate and means with standard deviation were calculated. The antioxidant activity of synthesized zinc doped cadmium sulfide NPs was evaluated by DPPH radical scavenging assay.

Using zinc doped cadmium sulfide nanoparticles with different concentration (10, 50, 100, 500 and 1000 µg/mL) and ascorbic acid with different concentration (10, 50, 100, 500 and 1000 µg/mL).

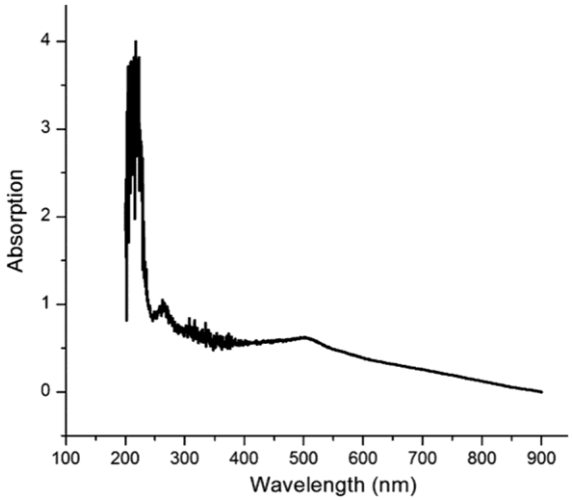

Fig. 13 — UV-Visible spectrum of zinc doped cadmium sulphide

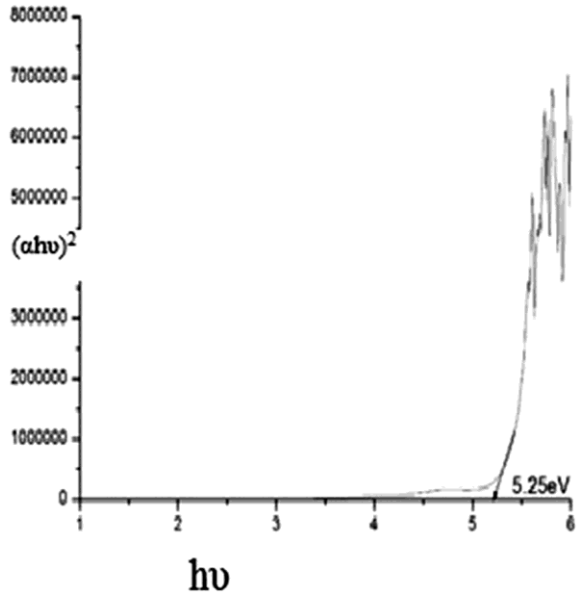

Fig. 14 — Optical band graph of zinc doped cadmium sulphide

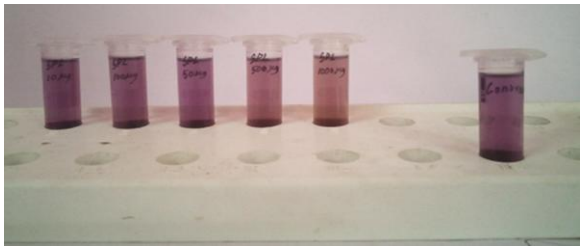

Fig. 15 — Anti-Oxidant property of Zn:CdS nanoparticles

Table 2 — Anti-oxidant analysis for Zn:CdS nanoparticle (sample)

Concentration µg	Absorbance	% inhibition
10	1.058	3.46
50	0.954	12.96
100	0.723	34.03
500	0.618	43.62
1000	0.542	50.54

Table 3 — Anti-Oxidant analysis for ascorbic acid (standard)

Concentration µg	Absorbance	% inhibition
10	1.034	5.65
50	0.642	41.42
100	0.209	80.93
500	0.067	93.88
1000	0.058	94.71

Table 4 — Anti-Oxidant analysis result

Compound	DPPH assay (IC_{50} µg)
SPL	877.69
Ascorbic acid	5.12

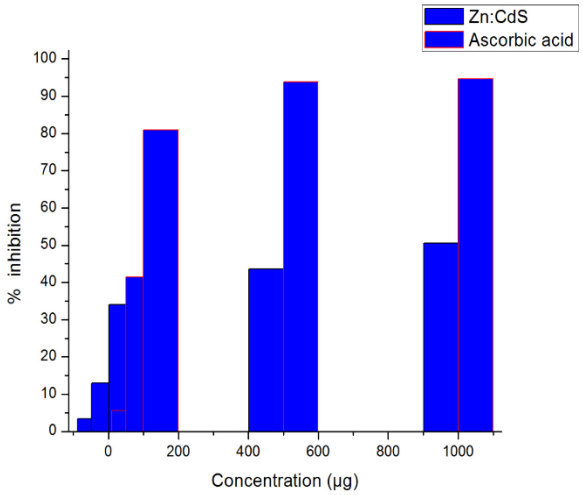

Graph 1 — Anti-oxidant property of zinc doped cadmium sulfide

Ascorbic acid was used as a positive control. The results obtained are summarized in Tables 2, 3 and 4. The Figure characterized in 15 and graph 1 respectively. We observed significant shift in the DPPH radical scavenging ability for studied samples. The scavenging ability increased in a dose dependent manner. The recorded scavenging ability for the lowest concentration of the synthesized Zn:CdS NP (10 µg/mL) was 4.23 ± 1.04 and this scavenging ability was increased to 70.90 ± 20.08. When concentration was increased to 250 µg/mL (average IC50 – 877.69). Zinc doped cadmium sulfide nanoparticle synthesis, characterization and antioxidant activities, were reported .

Conclusion

While comparing sample I, II and III, It have slight variation in stretching vibration around 1500 cm^{-1}. It may due to absorption of water molecule on the surface of nanocompound. When increase the concentration of zinc, it produce rough surface area. The result differ in each sample I, II and III. The crystalline grain size increases by increasing the concentration of Zn composition in sample I, II and III respectively. JCPDS confined that, Zinc doped cadmium sulfide nanoparticles shows hexagonal crystal arrangement. We observed that from SEM analysis, the particles are uniformly distributed. The SEM images of Zn doped CdS nanoparticle confirms the being of very small sized crystalline nanoparticle. The particle size and distribution of nanoparticle mainly depends upon the dopant concentration. When the concentration of Zn is increased, the structure of CdS becomes cluster form. Morphologies of nanoparticles can also be explained by the transmission electron microscopy image. It displays that, nano particles have rough surface area, which explains the catalysis application of product. It also explain the size of zinc doped cadmium sulfide nanoparticles lies between 2-14 nm. It displays crystalline arrangement of product by appearing lines in TEM image. The value obtained from TEM are in good agreement with the values obtained from XRD. The selected area electron diffraction (SAED) patterns were clearly shows rings, substantiating polycrystallinity of the samples. UV-Visible spectrum of zinc doped cadmium sulfide nanoparticles explains that, the wavelength of samples is 230 nm, which is blue shifted. This is because of quantum confinement effect.

Anti-oxidant activity of zinc doped cadmium sulfide nanoparticles was studied using DPPH (1,1-diphenyl-2-picrylhydrazyl) radical scavenging assay method. Zinc avail in ionic form (May presences of Zn^{2+} or Zn^{+}), which undergoes reaction with DPPH. Anti-oxidant activity were confirmed by color changes as well as absorption value. From this experiment we conclude that, zinc doped cadmium sulfide nano particles have 517 nm of absorption. The absorption value of nanoparticles depends on inhibition ratio of sample.

Acknowledgement

The author thanks VIT University, permiting me for analysis of samples.

References

1 Dona J M & Herrero J, *Thin films*, 5 (2002) 268.

2 Chandra T & Bhushan S, *J Mater Sci*, 39 (2004) 303.

3 Zeiri L, Patla I, Acharya S, Golan Y & Efrima S, *J Phys Chem*, 11 (2012) 231.

4 Awodugba A O & Adedokun O, *Pac J Sci Technol*, 12 (2011) 334.

5 Kim D S, Cho Y J, Park J, Yoon J, Jo Y & Jung M, *J Phys Chem*, 23 (2007) 56.

6 Celalettin B M & Orhan N, *Thin Films*, 18 (2010) 125.

7 Oztas M & Bedir M, *J Appl Sci*, 4 (2005) 67.

8 Illican S, Caglar Y & Caglar M, *Physica Macedonica*, 43 (2006) 173.

9 Pouretedal H R, Eskandari H, Keshavarz M H & Semnani A, *Acta Chem Slov*, 56 (2006) 348.

10 Becker W G & Bard A G, *J Phys Chem*, 87 (1983) 4888.

11 Awika J W, Rooney L W, Wu X, Prior R L & Zevallos L C, *J Agric Food Chem*, 51 (2003) 6657.

12 Holda A, Rodzik A, Mielnikow A A & Zukowski P W, *Phys Stat Sol* B, 189 (2009) 453.

13 Brus L E, *J Chem Phys*, 79 (1983) 5566.

14 Kaeble E F, *Handbook of X-rays*, (McGraw- Hill, NewYork, 1967)

15 O Donnell K P, Lee L M & Watkins G D, *J Phys C solid state phys*, 16 (1983) 723.

16 Muruganandam S, Anbalagan G & Murugadoss G, *Nanoscience*, 4 (2014) 1013.

17 Bhainsa K C & D'Souza S F, *Colloids Surf B*, 47 (2006) 160.

18 Cavall J F, Tomi F, Bernardini A F & Casanova J, *Phytochemical Anal*, 15 (2004) 275.

19 Santhoshkumar T, Rahuman A A, Jayaseelan C, Rajakumar G, Marimuthu S & Kirthi AV, *Asian Pac J Trop Med*, 7 (2014) 968.

20 Balaji D S, Basavaraja S, Deshpande R, Bedre D, Mahesh B K, Prabhakar A & Venkataraman M, *Colloids Surf B*, 1 (2009) 88.

21 Rehman A, Prabhakar B T, Vijay B R, Aditya S J & Ramesh C K, *J Appl Pharm Sci*, 7 (2011) 99.

22 Prasad C & Venkateswarlu P, *Indian J Adv Chem Sci*, 3 (2013) 208.

23 Braca A, Nunziatina De Tommasi, Lorenzo Di Bari, Cosimo Pizza, Mateo Politi & Ivano Morelli, *J Nat Prod*, 64 (2008) 892.

24 Chauhan R, Kumar A & Abraham J, *Sci Pharm*, 81 (2013) 607.

25 Azad B & Banerjee A, *Pharm Innov*, 7 (2014) 77.